Synthesis, controllable luminescence and energy transfer of $GdTaO_4$: Dy^{3+}, Eu^{3+} phosphors

Zhe Qiu [1, a], Shangrui Nan [1, b], Guixia Liu [1, c]

[1] School of Chemistry and Environmental Engineering, Changchun University of Science and Technology, Changchun 130022, P.R.China.

[a] 1499144305@qq.comcom, [b] 1948654365@qq.com, [c] liuguixia22@163.com

Abstract. In this study, Eu^{3+} and Dy^{3+} co-doped tantalum phosphor ($GdTaO_4$: Eu^{3+}/Dy^{3+}) was prepared by the sol-gel method, achieving controllable light emission across chromatic coordinates from green to orange-red wavelengths. The wide and intense photoluminescent excitation (PLE) band in the 200 nm-470 nm range is derived from the superposition of Dy^{3+} and Eu^{3+} excitation wavelengths, which means that it can be used for ultraviolet (UV) LED devices. At 352nm excitation, the phosphors emit blue, yellow and red light at 482 nm, 578 nm and 613 nm corresponded to the characteristic emission of Dy^{3+} and Eu^{3+}, further indicating that white light emission can be achieved with ultraviolet chip excitation. The luminescence color of the sample can be changed by modifying the doping ratio of Dy^{3+}/Eu^{3+}. The energy transfer efficiency $Dy^{3+}\rightarrow Eu^{3+}$ is calculated. These results deliver critical guidelines for developing multichromatic phosphors with adjustable emission characteristics.

Keywords: Phosphor; Energy transfer; luminescence.

1. Introduction

As the economy advances rapidly and people's living standards continue to improve steadily, more and more equipment is difficult to meet the application of people in daily life, among which the upgrading of energy-saving lighting system is the focus of people's research. The implementation of solid-state illumination technology utilizing rare-earth activated phosphors have emerged as a critical research frontier, particularly for energy-efficient lighting systems[1]. Phosphor conversion type white light emitting diodes(pc-WLEDs), regarded as promising lighting materials, are widely used in daily life, agriculture, industry, and other fields due to their environmental friendliness, high stability and long lifespan. However, the low color rendering performance and high energy consumption of pc-WLEDs have greatly reduced their application in daily life. Improving energy transfer efficiency of the phosphors used in pc-WLEDs can effectively improve this problem. Therefore, the preparation of novel phosphors with high luminescence properties is currently the top priority of research[2].

Tantalate as a phosphor substrate material has a highly symmetrical crystal structure (such as perovskite type), the symmetric perovskite structure can effectively reduce lattice distortion while optimizing the coordination environment for rare earth ions, thereby enhancing energy transfer efficiency [3]. The TaO_4^{3-} group can absorb ultraviolet light and generate a charge transfer band to make doping ions produce characteristic emissions and enhanced luminescence intensity and quantum yield. The strong Ta-O covalent bond can give the material with excellent thermal stability, making it highly suitable for high-power LED and laser lighting applications. Moreover, tantalate has a wide band gap (~4 eV), which can reduce the absorption of the matrix on the emitted light[4].

The luminescence properties depend not only on the substrate material but also on the doped ions. Eu^{3+} usually displays red light in the spectra[5]. When the non-inversion symmetry site is occupied, the $^5D_0\rightarrow{}^7F_2$ transition dominates the emission spectrum, producing red emission of about 613 nm[6]. Dy^{3+} doped phosphors usually show characteristic emission of blue and yellow light due to $^4F_{9/2}\rightarrow{}^6H_{15/2}$ transitions (482 nm) and $^4F_{9/2}\rightarrow{}^6H_{13/2}$ transitions (578 nm)[7]. In the case of co-doping of these two ions, the luminous color be changed by modifying the concentration ratio of Dy^{3+}/Eu^{3+}, so that the light color can be adjusted. The phosphors have been prepared by many methods[7-8].

However, the traditional solid-state high-temperature method results in uneven particle size, which affects color purity and other problems, so it is urgent to explore other synthesis method[9-11].

Here, The $GdTaO_4$:0.02Dy^{3+}, yEu^{3+} (y = 0.01-0.05) phosphors were effectively prepared using the sol-gel approach. The phosphor's luminescence properties and crystal structure were investigated and characterized. The light color can be adjusted by different doping ratio of Dy^{3+}, Eu^{3+}. In addition, the energy transfer was discussed in detail and the luminescence mechanism was studied in depth.

2. Experimental

2.1 Chemicals

Chemicals including Tantalum oxide (Ta_2O_5, 99.99%), Europium oxide (Eu_2O_3, 99.99%), Gadolinium oxide (Gd_2O_3, 99.99%), Ethylene glycol (EG, 96%), Concentrated nitric acid (HNO_3, 65%), and Hydrofluoric acid (HF, A.R.) were procured from Aladdin (Shanghai, China). All chemicals were not further purified before usage.

2.2 Synthesis of rare earth nitrates

Firstly, The following solutions were prepared: 0.1 mol/L $Gd(NO_3)_3$, 0.05 mol/L of $Dy(NO_3)_3$ and $Eu(NO_3)_3$: A certain amount of solid Gd_2O_3, Dy_2O_3 and Eu_2O_3 was placed in a 100 ml beaker, then a certain amount of HNO_3 was added to the beaker and slowly heated until the rare earth oxides were completely dissolved on the magnetic stirring. After continuous heating and stirring, the excess HNO_3 were evaporated, the rare earth nitrate solutions were cooled and crystallized, and deionized water was added to stir to dissolve it again. Finally, it was transferred to a volumetric bottle.

2.3 Synthesis of GdTaO4:Dy3+, Eu3+ phosphors

The phosphors were prepared by sol-gel method, taking $GdTaO_4$:0.02Dy^{3+}, 0.03Eu^{3+} as an example: First, 0.5 mmol of Ta_2O_5 was completely dissolved with HF, and then white precipitate will be generated after dropping ammonia water, until the solution pH value reaches 9. Washed the precipitate several times with deionized water to ensure that excess F^- was removed. Then, transferred it to a beaker and added 1.153 g citric acid under stirring conditions to dissolve it fully. At 50℃, 2 mL H_2O_2 was added until the solution was clarified, and then 1.0 mL EG was added. Added appropriate amount of $Gd(NO_3)_3$, $Dy(NO_3)_3$ and $Eu(NO_3)_3$ solutions to the beaker, then stirred at 85℃ to evaporate the excess water and formed a light yellow high-viscosity wet gel. The gel was transferred to the crucible and stored at 180℃ for 2 hours, then moved to a tube furnace and maintained at 500℃ for 3 hours., and the final grain-brown solid was ground into fine powder, and the white powder sample was obtained by calcining at 1100℃ for 5 h. The synthesized process of other samples was the same as that of the above phosphors, except that different concentrations of rare earth ions were used.

2.4 Characterizations

The phase structure of the samples was characterized using a Ruker D8Advance X-ray diffractometer (XRD) fitted with Cu-Kα radiation (incident wavelength λ = 0.15406 nm). The scanning step and continuous scanning 2θ angle range were 0.02° and 10°-90°. The sample composition was determined using energy dispersive X-ray spectroscopy (EDS), and sample morphology was described using scanning electron microscopy (SEM). The HITACHI F-7000 spectrometer (produced by Hitachi, Japan) was employed to measure the PLE and PL spectra, along with the luminescence lifetimes. The operating voltage was 700 V and the excitation light source was 150 W xenon lamp.

3. Results and discussion

3.1 Structure, morphology and composition analysis

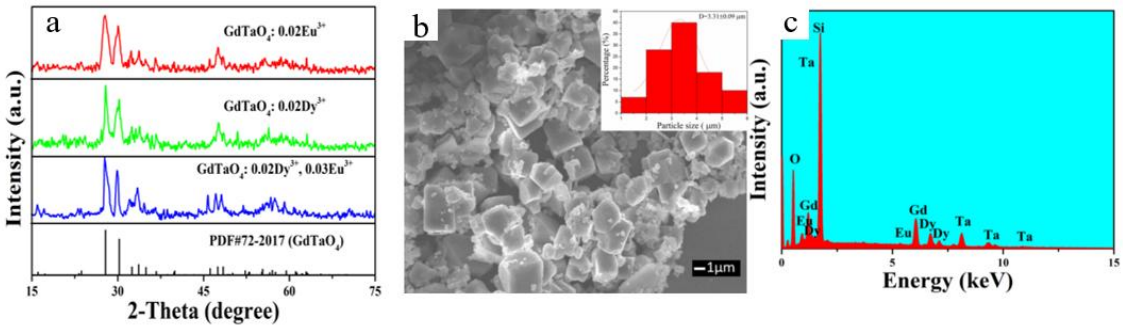

Fig. 1(a) XRD patterns of $GdTaO_4$:0.02Dy^{3+}, $GdTaO_4$:0.02Eu^{3+} and $GdTaO_4$:0.02Dy^{3+}, 0.03Eu^{3+} samples, and the corresponding standard data of $GdTaO_4$ (PDF#72-2017), (b) SEM image of $GdTaO_4$:0.02Dy^{3+}, 0.03$Eu^{3+}$and (c) EDS spectrum of $GdTaO_4$:0.02Dy^{3+}, 0.03Eu^{3+} sample, the illustration is the particle diameter diagram.

The XRD patterns of samples $GdTaO_4$:0.02Dy^{3+}, $GdTaO_4$:0.02Eu^{3+} and $GdTaO_4$:0.02Dy^{3+}, 0.03Eu^{3+} are displayed in Fig. 1(a). Characteristic peaks of the samples correspond to the standard card of GdTaO4. (PDF # 72-2017) with the lattice parameters a = 5.36 Å, b = 5.51 Å, c = 5.17 Å, and z = 2. This indicates that the phosphors have been successfully prepared. Since the ionic radii of Gd^{3+} (r = 0.938 Å), Dy^{3+} (r = 0.923 Å), and Eu^{3+} (r = 0.947 Å) are similar, the doped rare earth ions replace the position of Gd^{3+} ions in the matrix. In Fig. 1(b) and (c), $GdTaO_4$:0.02Dy^{3+} 0.03Eu^{3+}samples were selected for scanning electron microscopy testing and further EDS detection. The phosphor in Fig. 1(b) shows a uniformly distributed blocky structure, and there are some irregular structures on the surface of the sample, which may be caused by high temperature. The illustration shows that the average size of the sample is 3.31 μm. EDS spectrum analysis in Fig. 1(c) shows that the sample consists of Gd, Ta, O, Dy, Eu and other elements (among which the Si element comes from the silicon wafer), which once again proves the successful doping of Dy^{3+} and Eu^{3+}.

3.2 Optical properties

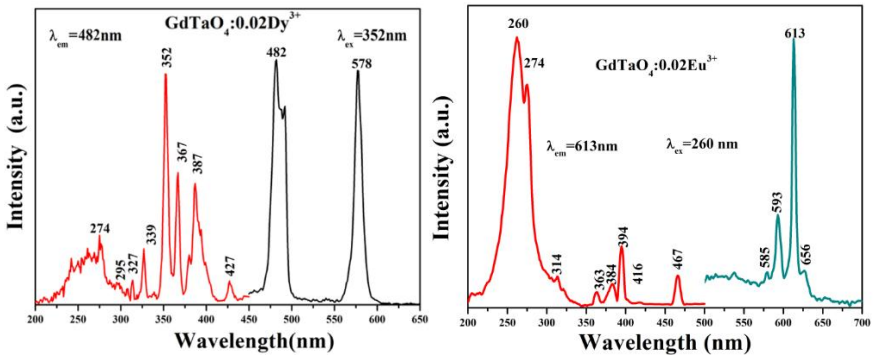

Fig. 3PLE and PL spectra of $GdTaO_4$: 0.02Dy^{3+}(a) and $GdTaO_4$:0.02Eu^{3+} (b).

The excitation and emission spectra for $GdTaO_4$:0.02Dy^{3+} can be observed in Figure 3(a). From the figure, it is evident that in a wavelength of 482 nm for monitoring, there is a wide excitation band (210-330 nm) resulted from the charge transfer of O^{2-}-Dy^{3+} and O^{2-}-Ta^{5+}. The excitation peaks at 274 nm and 314 nm originate from the Gd^{3+} transitions of $^8S_{7/2} \rightarrow {}^6I_{7/2}$ and $^8S_{7/2} \rightarrow {}^6P_{7/2}$, proving that there is energy transfer from Gd^{3+} to Dy^{3+}. Under excitation at 352nm, it is evident that the 482 nm and 578 nm emission peaks of Dy^{3+} correspond to the transitions of $^4F_{9/2} \rightarrow {}^6H_{15/2}$ and

$^4F_{9/2} \rightarrow {}^6H_{13/2}$. The excitation and emission spectrum of $GdTaO_4:0.02Eu^{3+}$ are displayed in Fig. 3(b). Monitoring at 613 nm, the process of charge transfer between O^{2-} and Eu^{3+}, as well as O^{2-} and Ta^{5+}, the material produces a wide absorption band at 260 nm (210-300 nm), indicating that the TaO_4^{3-} group can transfer the absorbed energy to Eu^{3+}. The detection of different absorption peaks at 274 and 314 nm confirms the effective energy transfer of Gd^{3+} to the activator of Eu^{3+}. In addition, a series of absorption peaks at 300 to 450 nm correspond to the $^7F_0 \rightarrow {}^5D_4$, $^5G_4$, $^5L_6$, $^5D_3$ and $^5D_2$ transitions of Eu^{3+}. After doping Dy^{3+}, the emission peak of Eu^{3+} is enhanced, indicating that Eu^{3+} mainly holds the non-inverse symmetric center environment in $GdTaO_4:Eu^{3+}$ phosphor[12].

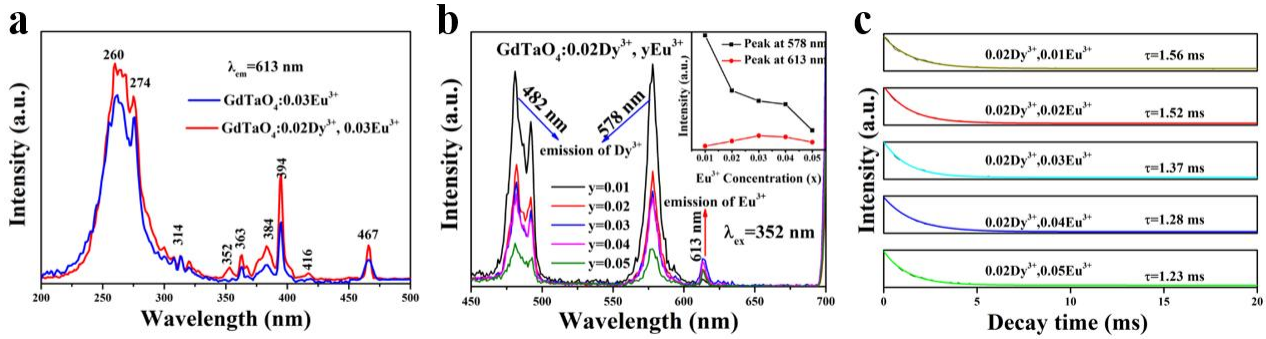

Fig. 4(a) Excitation spectra of $GdTaO_4:0.03Eu^{3+}$ and $GdTaO_4:0.02Dy^{3+}$, $0.03Eu^{3+}$, (b) Emission spectra of $GdTaO_4:0.02Dy^{3+}$, yEu^{3+} (y = 0.01 - 0.05) excited by 352 nm, illustration is 578 and 613 nm emission intensity corresponding to Eu^{3+} content,(c) Fluorescence lifetime decay curves for $GdTaO_4:0.02Dy^{3+}$, yEu^{3+} (y = 0.01 - 0.05) phosphors (λ_{ex} =352 nm, λ_{em} =482 nm).

The excitation spectra of samples $GdTaO_4:0.03Eu^{3+}$, $GdTaO_4:0.02Dy^{3+}$, $0.03Eu^{3+}$ shown in Fig. 4(a). Under 613 nm monitoring, 200-300 nm excitation peaks are derived from O^{2-} - Ta^{5+} and O^{2-} - Eu^{3+} charge transfer bands (CTB), and 350 – 470 nm excitation peaks are derived from excitation peaks of Gd^{3+}, Dy^{3+} and Eu^{3+} ions. In addition, In the 363 – 387 nm range, the excitation peaks of Dy^{3+} and Eu^{3+} ions partially overlap [13]. Therefore, the peak intensity of Eu^{3+} is increased after doping Dy^{3+}. Fig. 4(b) displays the PL spectra at 352 nm excitation. The figure illustrates characteristic emission bands corresponding to Eu^{3+} (613 nm) and Dy^{3+} (482 nm, 578 nm). The highest emission intensity is achieved when y reaches 0.03, after which it starts to decline until the concentration is quenched. The Dy^{3+} emission peak intensity continues to declining. The above results show that the existence of energy transfer processes. Fig. 4(c) displays the fluorescence lifetime of Dy^{3+} ion under 482 nm monitoring and 352 nm excitation. The experimental data can be modeled by utilizing the formula (1)[14].

$$I = I_0 + Ae^{-t/\tau} \quad (1)$$

Where I is the PL intensity at t, I_0 represents the PL intensity at $t = 0$, τ represents the luminescence lifetime. As shown in Fig. 4(c), with increasing Eu^{3+} concentration, the luminous lifetime of Dy^{3+} is 1.56, 1.52, 1.37, 1.28 and 1.23 ms, showing a gradually decreasing trend. The above results prove the energy transfer process of $Dy^{3+} \rightarrow Eu^{3+}$.

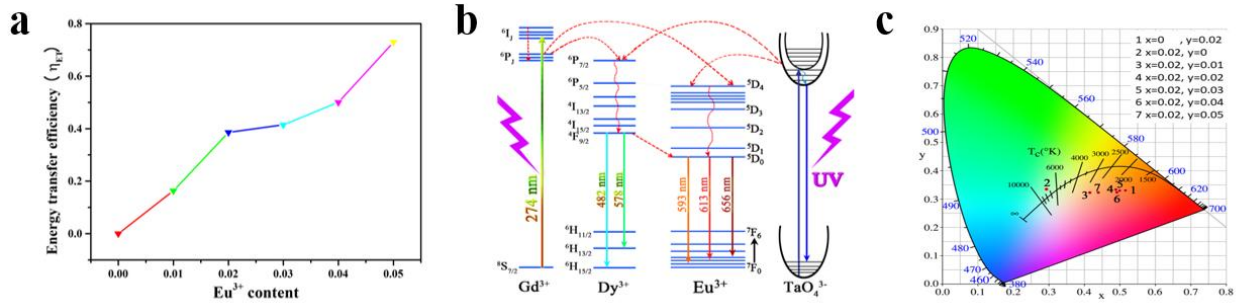

Fig. 5(a) Energy transfer efficiency from Dy^{3+} to Eu^{3+} in $GdTaO_4$:0.02Dy^{3+}, yEu^{3+} (y = 0.01-0.05) (λ_{ex} = 352 nm), (b) The emission mechanism of $GdTaO_4$:Dy^{3+}, Eu^{3+} phosphors, (c) CIE chromaticity diagram of $GdTaO_4$:xDy^{3+}, yEu^{3+} (x = 0-0.02, y = 0-0.05) upon 275 nm excitation.

The efficiency of energy transfer from Dy^{3+} to Eu^{3+} in the $GdTaO_4$ matrix can be calculated by (2)

$$\eta_{ET} = 1 - \frac{I_S}{I_{SO}} \tag{2}$$

where I_{s0} is the $GdTaO_4$:0.02Dy^{3+} emission intensity and I_s is the emission intensity of Dy^{3+} when Dy^{3+} and Eu^{3+} ions are doped. As can be seen in Fig. 5(a), when Eu^{3+} doping concentration is 0.05, the energy transfer efficiency reaches 73%. Figure 5(b) illustrates that under 274 nm excitation, the electrons of $Gd^{3+}$are excited, and then the electrons are transferred to the $^6P_{7/2}$ level of Dy^3 and the $^5D_4$ level of Eu^{3+}. The electrons of Dy^{3+} ions relax from $^6P_{7/2}$ to $^4F_{9/2}$, then transfer to $^6H_{15/2}$ and $^6H_{13/2}$. In addition, when the electrons of Dy^{3+} are excited to the excited state, they also transfer some of the absorbed energy to Eu^{3+}. The electrons transition from $^5D_0$ to ^7F_J (J=1,2,3), the Eu^{3+} ion emits red light at 593, 613 and 656 nm. At the same time, under ultraviolet light, the TaO_4^{3-} in the matrix will also transfer energy to Dy^{3+} and Eu^{3+} ions, resulting in the characteristic emission of Dy^{3+} and Eu^{3+} ions. Figure 5(c) shows with the increase of Eu^{3+} ion concentration, its color coordinates move from the blue region toward the red regions, and the results prove the color of the emitted light can be adjusted. Therefore, under a single wavelength excitation of 275 nm, $GdTaO_4$:xDy^{3+}, yEu^{3+} phosphor can be used in WLED applications.

4. Conclusion

In this study, The $GdTaO_4$:0.02Dy^{3+}, yEu^{3+} (y = 0.01-0.05) phosphor was effectively prepared using the sol-gel approach. Under monitor at 613 nm, the absorption peak of Gd^{3+} ion and O^{2-} - Ta^{5+} charge transfer band can be shown in excitation spectra. Energy can be transferred to Dy^{3+} and Eu^{3+} ions by both TaO_4^{3-} and Gd^{3+}. At 352nm excitation, Dy^{3+} ions emit blue and red light, and Eu^{3+} ions emit red light. The sample's color shift from the blue to the white and red regions as the Eu^{3+} doping content increases. The results show that the prepared $GdTaO_4$:Dy^{3+}, Eu^{3+} phosphor has important underlying application value in this domain of LED display, biological tissue imaging and color display.

Acknowledgements

This work was supported financially by the Science and Technology Development Planning Project of Jilin Province (20240101075JC).

Conflicts of Interest

The authors declare no conflicts of interest regarding the publication of this paper.

References

[1] Hongli Du, Wenfei Shan, Liying Wang, et al. Optimization and complexing agent-assisted synthesis of green SrAl2O4: Eu2+, Dy3+ phosphors through sol–gel process. Journal of Luminescence, 2016, 176: 272-277.

[2] Chao Dou, Shengqiang Liu, Fangyi Zhao, et al. Enhancing external quantum efficiency of blue-emitting phosphor Ba (K)-β-Al2O3: Eu2+ by lattice site engineering for full-spectrum lighting. Inorganic Chemistry, 2023, 62(25): 10021-10028.

[3] Rui Yuan, Meng Huang, Fei Zheng, et al. Rapid, convenient and low-energy preparation of spherical rare earth doped YAG phosphors by a laser sintering method. Journal of Materials Chemistry C, 2019, 7(42): 13070-13079.

[4] Nan Yang, Zhuo Li, Ziwang Zhang, et al. A highly thermal-stable red-emitting tantalate phosphor for WLED and multiple-mode optical temperature sensor dual-applications. Ceramics International, 2024, 50(4): 6880-6891.

[5] Xue Huang, Wentao Zhang, Xiaomeng Wang, et al. Optical characteristics and energy transfer between Eu3+ and Dy3+ in Na2CaSiO4: Dy3+, Eu3+ white-emitting phosphor. Journal of Alloys and Compounds, 2021, 873: 159803.

[6] Xiaoxuan Fan, Lirong Xu, Wen Liu, et al. Energy transfer in dual-emission LiY6(BO3)3O5: Bi3+, Eu3+ phosphors for temperature sensing applications. Ceramics International, 2024, 50(18): 32583-32590.

[7] Conglin Liu, Youkui Zheng, Yue Qin, et al. Study on a highly thermostable Dy3+activated borophosphate phosphor. Inorganic Chemistry, 2024, 63(14): 6483-6492.

[8] Daoyuan Ma,Yunzheng Liu,Wenfa Fang, et al. The structure transition and luminescence performance of a high moisture resistant KNaNbOF5: Mn4+ red phosphor. Journal of Materials Chemistry C, 2025, 13(3): 1378-1387.

[9] Haokun Yan, Runfu Li, Liuzhen Feng, et al. Simultaneous negative thermal quenching luminescence of upconversion and downshifting processes in Al2(WO4)3: Yb3+/Er3+ phosphors with low thermal expansion. Journal of Materials Chemistry C, 2024, 12(32): 12353-12362.

[10] Yifan Liu, Yabin Wang, Xiaoqing Pei, et al. Optical properties of Eu3+/Dy3+ doped BaY2(MoO4)4 white light phosphor. Optical Materials, 2024, 157: 116350.

[11] Yuefeng Qiu, Ruirui Cui, Min Zhang, et al. Dual-emitting Dy3+/Eu3+ co-doped SrLaGaO4 phosphor: tunable luminescence, energy transfer and ratiometric temperature sensing. Journal of Molecular Structure, 2024, 1304: 137622.

[12] Junhua Hong, Yue Liu, Yingchao Xu, et al. Luminescence properties and energy transfer study of color temperature tunable CaSrSiO4: Dy3+, Eu3+ white phosphors. Optical Materials, 2024, 149: 115033.

[13] Xiaoxuan Fan, Lirong Xu, Wen Liu, et al. Energy transfer in dual-emission LiY6 (BO3) 3O5: Bi3+, Eu3+ phosphors for temperature sensing applications. Ceramics International, 2024, 50(18): 32583-32590.

[14] Xiang Lv, Ning Guo, Wenzhen Lv, et al. Regulating luminescence thermal quenching of praseodymium-doped niobo-tantalate phosphor through intervalence charge transfer band displacement. Inorganic Chemistry, 2023, 62(38): 15747-15756.